



HAL
open science

Protocol for evaluating in vivo the activation of the P2RX7 immunomodulator

Serena Janho Dit Hreich, Thierry Juhel, Paul Hofman, Valérie Vouret-Craviari

► **To cite this version:**

Serena Janho Dit Hreich, Thierry Juhel, Paul Hofman, Valérie Vouret-Craviari. Protocol for evaluating in vivo the activation of the P2RX7 immunomodulator. *Biological Procedures Online*, 2023, 25 (1), pp.1. 10.1186/s12575-022-00188-6 . hal-04188434

HAL Id: hal-04188434

<https://hal.science/hal-04188434>

Submitted on 25 Aug 2023

HAL is a multi-disciplinary open access archive for the deposit and dissemination of scientific research documents, whether they are published or not. The documents may come from teaching and research institutions in France or abroad, or from public or private research centers.

L'archive ouverte pluridisciplinaire **HAL**, est destinée au dépôt et à la diffusion de documents scientifiques de niveau recherche, publiés ou non, émanant des établissements d'enseignement et de recherche français ou étrangers, des laboratoires publics ou privés.

1 **Protocol for evaluating *in vivo* the activation of**
2 **the P2RX7 immunomodulator**

3

4 Serena Janho dit Hreich^{1,2}, Thierry Juhel¹, Paul Hofman^{1,2,3,4}, Valérie Vouret-
5 Craviari^{1,2}

6 1. Université Côte d'Azur, CNRS, INSERM, IRCAN, 28 avenue de Valombrose, 06108
7 Nice, France

8 2. FHU OncoAge, Pasteur Hospital, 30 voie Romaine, 06001, Nice, France

9 3. Laboratory of Clinical and Experimental Pathology and Biobank, Pasteur Hospital, 30
10 voie Romaine, 06001, Nice, France

11 4. Hospital-Related Biobank (BB-0033-00025), Pasteur Hospital, 30 voie Romaine,
12 06001, Nice, France

13

14

15 Corresponding authors: serena.janho-dit-hreich@etu.univ-cotedazur.fr, valerie.vouret@univ-
16 [cotedazur.fr](mailto:valerie.vouret@univ-cotedazur.fr)

17

18

1 **Abstract**

2 **Background:** P2RX7 is a purinergic receptor with pleiotropic activities that is activated by
3 high levels of extracellular ATP that are found in inflamed tissues. P2RX7 has
4 immunomodulatory and anti-tumor properties and is therefore a therapeutic target for various
5 diseases. Several compounds are developed to either inhibit or enhance its activation.
6 However, studying their effect on P2RX7's activities is limited to *in vitro* and *ex vivo* studies
7 that require the use of unphysiological media that could affect its activation. Up to now, the
8 only way to assess the activity of P2RX7 modulators on the receptor *in vivo* was in an indirect
9 manner.

10 **Results:** We successfully developed a protocol allowing the detection of P2RX7 activation *in*
11 *vivo* in lungs of mice, by taking advantage of its unique macropore formation ability. The
12 protocol is based on intranasal delivery of TO-PRO™-3, a non-permeant DNA intercalating
13 dye, and fluorescence measurement by flow cytometry. We show that ATP enhances TO-
14 PRO™-3 fluorescence mainly in lung immune cells of mice in a P2RX7-dependant manner.

15 **Conclusions:** The described approach has allowed the successful analysis of P2RX7 activity
16 directly in the lungs of WT and transgenic C57BL6 mice. The provided detailed guidelines and
17 recommendations will support the use of this protocol to study the potency of pharmacologic
18 or biologic compounds targeting P2RX7.

19

20 **Keywords:** P2RX7, P2X7 receptor, purinergic receptors, ATP, macropore, TOPRO-3, activity

21

1 **Background**

2 The purinergic P2X family of receptors is a family of 7 receptors that are all activated by
3 extracellular ATP (eATP) with various affinities. Unlike the other 6 receptors, P2RX7 requires
4 high levels of eATP (in the range of hundreds of micromolar) to be activated. Such levels of
5 eATP are found in inflamed tissues such as the tumor microenvironment or fibrotic sites [1].

6 P2RX7 is a receptor with pleiotropic activities. Its activation leads to calcium influx and
7 potassium efflux, a feature it shares with all members of the P2X family and that has been
8 shown to trigger activation of various signaling pathways [2]. However, P2RX7 has its own
9 particularities: its activation also leads to a macropore opening at the plasma membrane that
10 allows the non-selective entry of macromolecules (up to 900 Da) to the cell. Compromising
11 membrane integrity through macropore opening by a prolonged or sustained activation (over
12 1 hour) of P2RX7 could also lead to cell death[3]. Moreover, activation of P2RX7 leads
13 subsequently to the assembly of the NLRP3 inflammasome and the release of mature IL-1 β
14 and IL-18 from the cell [4].

15 Due to its ability to induce cell proliferation and death but also to modulate the immune
16 response, several approaches are undertaken to either inhibit or enhance its activation, by
17 engineering chemical molecules [5,6] or nanobodies [7] targeting the receptor. Three assays
18 are classically and routinely used to evaluate their ability to modulate P2RX7's activation,
19 based on the 3 hallmarks of P2RX7:

- 20 • Calcium influx: the goal is to measure intracellular calcium concentrations using cell
21 permeant fluorescent calcium indicators such as Fluo-4 AM or Fura 2. Calcium
22 concentration could be assessed by spectrophotometry, microscopy or flow cytometry.
23 Calcium influx could also be detected by measuring ion fluxes by electrophysiology
24 techniques such as patch-clamp.

- 1 • Macropore opening: To evaluate the opening of the macropores, non-permeant DNA
2 intercalating fluorescent dyes of high molecular weight (up to 900 Da) are used, such
3 as TO-PRO™-3 or Ethidium bromide. Fluorescence is assessed by
4 spectrophotometry, microscopy or flow cytometry.
- 5 • NLRP3 inflammasome activation is determined by checking adaptor protein ASC
6 oligomerization, caspase-1 cleavage or IL-1 β /IL-18 release. It is assessed by
7 immunofluorescence, western blot, flow cytometry or ELISA.

8 However, these assays are *in vitro* or *ex vivo*-based and rely on using unphysiological medias
9 that could interfere with P2RX7 activation. Indeed, the ionic composition of media is crucial.
10 ATP-induced cell death has been shown to be delayed in low-salt medias[8]. Moreover,
11 macropore formation is impacted by Na⁺, iodide, thiocyanate and chloride-enriched medias,
12 since increasing concentration of these ions inhibited ethidium uptake by cells[9]. Channel
13 opening is also affected by external anions such as glutamate that potentiates human P2RX7
14 activation whereas chloride and iodide decreased it [10]. Since P2RX7 activation hangs in the
15 balance of ions concentrations in media, measurement of its activation *in vitro* and its
16 translation *in vivo* can be not accurate. For example, under pathological conditions, glutamate
17 levels increase in the extracellular space during nerve injury, that could affect P2RX7
18 activation [11].

19 Since compounds targeting P2RX7 are tested *in vitro*, little is known on their impact on P2RX7
20 activities *in vivo*, i.e. in complete physiological conditions. Up to now, *in vivo* P2RX7 activation
21 state is only seen indirectly through eATP levels or IL-1 β /IL-18 production. Therefore, we
22 aimed at setting up a way to measure its activation *in vivo* and developed a protocol based on
23 intranasal delivery of TO-PRO™-3 and fluorescence measurement by flow cytometry.

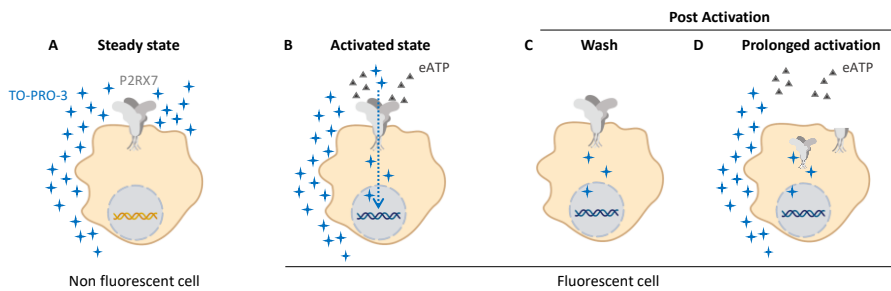
24

25

1 **Results**

2 **General strategy to measure P2RX7 activity *in vivo***

3 Since calcium influx is a common feature of P2X receptors and that NLRP3 assembly is a step
4 downstream of P2RX7 but also not specific to P2RX7, we opted to use macropore opening,
5 which directly represent the activation state of the receptor, as a readout for P2RX7 activity
6 (Fig. 1). Several dyes are available for measuring macropore opening. We opted to use the
7 TO-PRO™-3 dye (Invitrogen) since it is the most sensitive non-permeant DNA intercalating
8 dye and was shown to work best in flow cytometry [12].



9 **Fig. 1.** Activation of P2RX7 and macropore opening using TO-PRO™-3 dye

10 When the cell is in steady state (absence of eATP, membrane integrity) TO-PRO™-3 does not
11 enter the cell and the cell remains non fluorescent (Fig. 1A). In the presence of eATP, P2RX7
12 is activated and macropores are open, permitting the entry of TO-PRO™-3 into the cell. TO-
13 PRO™-3 binds to DNA and renders the cell fluorescent (Fig. 1B). Macropore formation is a
14 reversible mechanism. However, once P2RX7 is activated, the cell remains fluorescent since
15 TO-PRO™-3 has already bound to DNA, even if no eATP remains or if P2RX7 is internalized
16 [13,14] or cleaved [15] during a prolonged activation (Fig. 1C and D), allowing the detection
17 of P2RX7 activation at any point in time.

18 Channel opening and P2RX7-dependent calcium influx are detected few seconds after ATP
19 stimulation. However, detection of macropore formation is much slower due to the
20 incorporation of fluorescent dyes in DNA. and can take up to 1 hour to detect all activated

1 receptors [12]. We have previously shown in a time course experiment of ATP-induced TO-
2 PROTM-3 uptake that a range between 20 and 30 minutes post stimulation is the ideal time
3 point at which the TO-PRO-3 signal is well above background [5]. Moreover, since prolonged
4 activation of P2RX7 (over 1 hour) can also lead to cell death in a macropore-dependent
5 manner and since TO-PROTM-3 can also detect dead cells, it is crucial to add a Live/Dead
6 marker. Indeed, excluding dead cells to reduce background noise and macropore-unrelated
7 TO-PROTM-3 staining is important for accurate P2RX7-activation measurement. Therefore, to
8 detect P2RX7-related TO-PROTM-3 fluorescence and to rule out detection of ATP-induced cell
9 death, we chose to activate P2RX7 for 30 minutes *in vivo*.

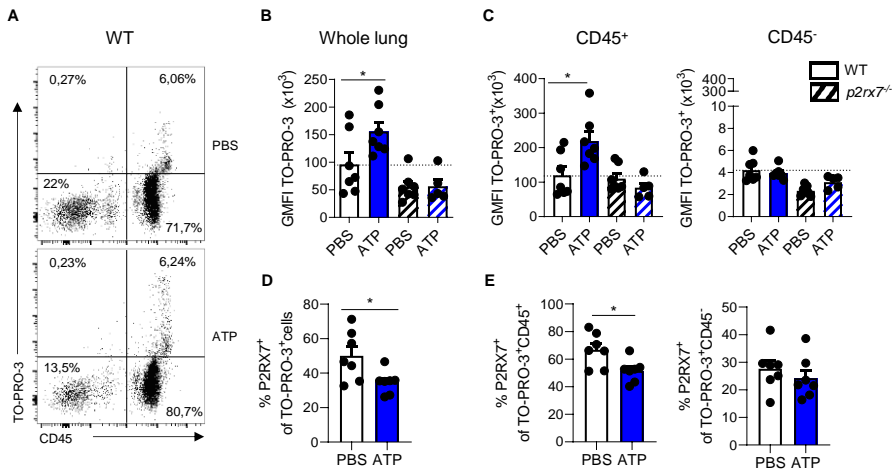
10 **ATP activates P2RX7 in the lung and increases *in vivo* TO-PROTM-3 fluorescence.**

11 We first analyzed TO-PROTM-3 fluorescence in the whole lung. We observed an increase of
12 fluorescence in WT mice receiving ATP compared to PBS (Fig. 2A and B), indicative of
13 macropore opening and therefore activation of P2RX7. In order to know if this increase is
14 specific of P2RX7, the experiment was also done on *p2rx7^{-/-}* mice, where the increase of TO-
15 PROTM-3 fluorescence in the ATP group was not observed and was similar to WT-PBS mice
16 (Fig. 2B). No difference was observed in the percentage of TO-PROTM-3 positive cells (supp
17 Fig. 1A-C). These results suggest that TO-PROTM-3 fluorescence after ATP administration
18 was specific to P2RX7 and indicative of its activation state.

19 To go further, we analyzed TO-PROTM-3 fluorescence in immune and non-immune cells. We
20 show that WT-ATP mice exhibit an enhanced fluorescence compared to WT-PBS mice only
21 in immune cells (Fig. 2C), and that was only observed in WT mice, demonstrating furthermore
22 the requirement of P2RX7 for the TO-PROTM-3 signal observed.

23 We also show that TO-PROTM-3⁺ cells express P2RX7. However, percentage of P2RX7⁺ cells
24 among TO-PROTM-3⁺ cells was decreased in ATP-mice (Fig. 2D and E), but not in TO-PROTM-
25 3⁺CD45⁻ cells (Fig. 2E). This is not surprising since it has been shown that sustained activation

- 1 of P2RX7 leads to the internalization of the receptor[14] or its cleavage [15] after its activation,
- 2 explaining the possibility of TO-PROTM-3⁺P2RX7⁻ cells.



3 **Fig. 2.** P2RX7 is activated *in vivo*

- 4 **A** Dotplot gated on live single cells of WT mice whole lungs
- 5 **B** GMFI of TO-PROTM-3⁺ cells in whole lung of WT and *p2rx7*^{-/-} mice.
- 6 **C** GMFI of TO-PROTM-3⁺ cells in CD45⁺ cells (left) and CD45⁻ cells (right) in WT and *p2rx7*^{-/-} mice
- 7 **D** Percentage of P2RX7⁺ cells among TO-PROTM-3⁺ cells,
- 8 **E** Percentage of P2RX7⁺ cells among TO-PROTM-3⁺CD45⁺ cells (left) and TO-PROTM-3⁺CD45⁻
- 9 cells (right). One point represents one mouse, data is represented as mean±SEM. Two-tailed
- 10 unpaired *t*-test. **p* < 0.05. WT: Wildtype, GMFI: geomean fluorescence intensity

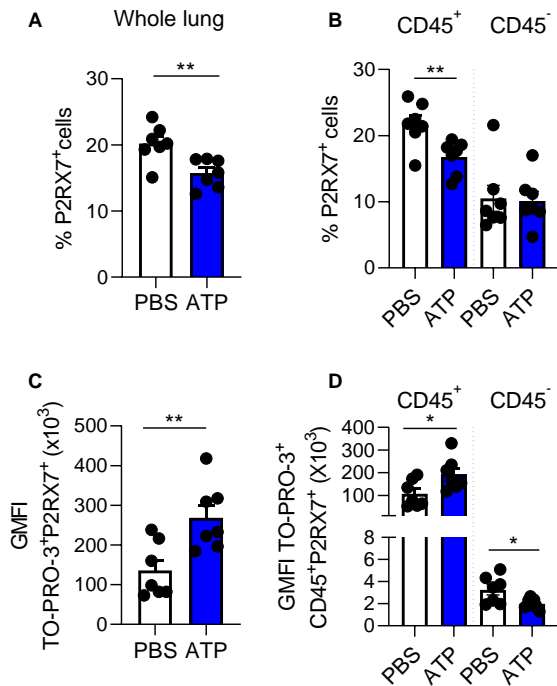
11

12 **P2RX7 is mainly expressed and activated in lung immune cells**

13 Since we observed a decrease of P2RX7 expression in TO-PRO-3⁺ cells (Fig. 2D and E), we
 14 investigated furthermore its expression in whole lungs of mice. We show that the expression
 15 of P2RX7 was decreased in all cells (Fig. 3A) but also in immune cells (Fig. 3B), supporting
 16 furthermore the idea of an internalization of P2RX7 after its activation. Moreover, we show
 17 that P2RX7 is more expressed by immune cells than non-immune cells (Fig. 3B). Even though

Commenté [V1]: In cells positive for TO-PRO-3

- 1 WT-ATP mice show a decrease of P2RX7 expression, P2RX7⁺ cells show a higher TO-
- 2 PROTM-3 fluorescence in all cells (Fig. 3C) and in immune cells (Fig. 3D), meaning that
- 3 P2RX7⁺ cells are indeed activated by ATP.



4

5 **Fig 3.** TO-PROTM-3 fluorescence is increased in P2RX7⁺ cells in WT mice

- 6 **A** Percentage of P2RX7⁺ cells in the whole lung of WT mice
- 7 **B** Percentage of P2RX7⁺ cells in CD45⁺ and CD45⁻ cells
- 8 **C** GMFI of TO-PROTM-3 in P2RX7⁺ cells
- 9 **D** GMFI of TO-PROTM-3 in P2RX7⁺CD45⁺ and P2RX7⁺CD45⁻ cells

10 One point represents one mouse, data is represented as mean±SEM. Two-tailed unpaired *t*-test.
 11 **p* < 0.05, ***p* < 0.01. WT: Wildtype, GMFI: geomean fluorescence intensity

12

1 Since TO-PRO™-3 fluorescence (Fig. 2C) and P2RX7 expression (Fig. 2E, Fig. 3B) were
2 unchanged after ATP delivery in CD45⁻ cells, we can speculate that P2RX7-expressing
3 immune cells are the main cells activated by ATP in the lung. However, we observed a
4 decrease of TO-PRO™-3 fluorescence in CD45⁻ P2RX7⁺ cells (Fig. 3D).

5

1 **Discussion**

2 This protocol was set up to assess P2RX7 activation *in vivo*, by taking advantage of its
3 property of macropore formation. Among P2X receptors, a permeability for large cations was
4 also described for P2RX2 and P2RX4. However, P2RX7 is activated by high concentrations
5 of eATP (0.5 to 1 mM), whereas P2RX2 and P2RX4 are activated by much lower
6 concentrations (3 to 10 μ M). Unlike P2RX7, P2RX2 and P2RX4 receptors desensitize after
7 ATP stimulation. Even though P2RX4 is broadly expressed in most tissues of the body, it is
8 preferentially localized in lysosomes where the acidity prevents its activation [16]. Based on
9 these properties, we hypothesized that the macropore activity of P2RX2 and P2RX4 will not
10 interfere with our assay. This is indeed the case since no increase in TO-PROTM-3 signal was
11 observed in *p2rx7^{-/-}* mice (Fig. 2B).

12 Our protocol allows the measurement of P2RX7 activation in lungs and is based on TO-
13 PROTM-3 uptake by cells and detection by flow cytometry. Flow cytometry was previously
14 shown as a sensitive tool to study P2RX7 activation *in vitro* [12] and is also efficient for analysis
15 of an *in vivo* activation of the receptor as shown in this study. Moreover, flow cytometry allows
16 the reduction of background noise by excluding non P2RX7-dependent TO-PROTM-3 staining
17 of dead cells. The other advantage of using flow cytometry is coupling TO-PROTM-3 with other
18 surface markers to distinguish P2RX7 activation at the single cell level. We only studied its
19 activation in immune versus non-immune cells, however, one can easily increase the number
20 of markers during the surface staining step to precisely identify the subtypes of immune and
21 non-immune cells activated by ATP.

22 To our knowledge, we show for the first time in a direct manner that P2RX7 is mainly activated
23 in lung immune cells of mice, as per an increase of TO-PROTM-3 fluorescence. P2RX7 has a
24 pro-inflammatory role since it releases IL-1 β and is at the etiology of inflammatory diseases.
25 Nonetheless, direct activation of the receptor i.e. calcium influx or macropore formation was
26 never assessed *in vivo*. However, expression of P2RX7 on hematopoietic cells [17,18], ATP

1 levels [19,20] and IL-1 β release [21,22] were shown *in vivo* to be important for airway
2 inflammation in mouse models. Even so, these experiments require the use of transgenic and
3 chimeric mice and do not evaluate the receptor activation status. Our protocol could be used
4 instead for accurate and easier assessment of the activation of P2RX7. We previously showed
5 using human tumor lung adenocarcinoma (LUAD) tissues that P2RX7 is expressed in tumor
6 associated immune cells whereas non-immune cells do not express P2RX7. Further, we
7 showed that the overall activity of P2RX7 is impaired by expression of the C-terminal domain
8 truncated P2RX7B receptor in immune cells [23]. Accordingly, we also show that ATP did not
9 enhance TO-PROTM-3 fluorescence in non-immune cells. Lung CD45⁻ cells comprise
10 endothelial cells, fibroblasts, and alveolar epithelial cells of type I (AEC I) and type II (AEC II).
11 They all express P2RX7 except for AEC II. It has been shown *in vitro* and *ex vivo* studies that
12 they express a functional receptor (macropore opening, calcium influx, IL-1 β release) [24,25]
13 but we do not seem to detect an activation *in vivo* with our protocol by measuring TO-PROTM-
14 3 fluorescence in CD45⁻ cells. This could be due to the lower levels of expression of P2RX7
15 in CD45⁻ cells than in CD45⁺ cells (Fig. 3B, supp Fig. 2B) and the heterogeneity of the
16 amplitude of its activation in these cells that is lost when looking at overall CD45⁻ cells. One
17 possible way to overcome this is to analyze TO-PROTM-3 fluorescence in each CD45⁻ cell type
18 by including specific markers. However, we could not exclude that the overall macropore
19 activity of P2RX7 is impaired by the expression of truncated splice variants as previously
20 described in mouse astrocytes [26]. Surprisingly, we observed that TO-PROTM-3 fluorescence
21 was decreased in P2RX7⁺CD45⁻ cells in ATP-mice (Fig 3D). It should be noted that the
22 intensity of TOPROTM-3 fluorescence in P2RX7-expressing CD45⁻ cells (Fig. 3D) is identical
23 to the background value observed in *p2rx7*^{-/-} mice (Fig 2C) accompanied by unchanged
24 P2RX7 expression (Fig 3B, supp Fig 2B). Thus, these observations support the background
25 signal of TO-PRO-3 fluorescence rather than an ATP-related effect.

26 We have also shown that the expression of P2RX7 was decreased in WT-ATP mice. P2RX7
27 activation by ATP stimulates membrane internalization [27] that results to the loss of

1 expression of many surface proteins[28,29] including P2RX7 [13,14]. Indeed, prolonged
2 stimulation with high levels of ATP results in decreased surface expression and internalization
3 of the receptor in RAW cells [14], Caski cells and HEK 293 transfected with the human P2RX7
4 [13], at least 15 to 30 minutes after its activation depending on the cell type. Decreased
5 expression of the receptor was also reported on human and mouse monocytes after sustained
6 stimulation with bzATP [30]. Moreover, it has been shown that sustained activation of P2RX7
7 induces its cleavage at the plasma membrane by MMP-2, starting 15 minutes after its
8 activation [15]. Altogether, these observations support the decrease of P2RX7 surface
9 expression in lungs of mice due to high levels of ATP administration and duration of P2RX7
10 activation in this study.

11 Even though this protocol successfully detects P2RX7 activation in the lungs, it can be
12 adapted for studying its activation in other organs by giving TO-PRO™-3 to the mice by
13 intravenous (i.v.) route. YO-PRO-1 (an analog of TO-PRO™-3) and propidium iodide (PI) are
14 also used to study macropore formation. They have been given i.v. in mice and rats to study
15 *in vivo* cell death in lungs [31,32], brain [33,34] and liver [35]. However, TO-PRO™-3's time
16 to access and penetrate the organ of interest should be carefully assessed in order to study
17 the activation of P2RX7.

18 To go further, this protocol could also be helpful to determine the *in vivo* efficacy of compounds
19 targeting P2RX7, to potentially adapt their administration route or their dosage or even to
20 identify the targeted cell type of the compounds. HEI3090 is a novel positive modulator of
21 P2RX7 that enhances calcium influx, macropore opening and IL-18 release, as determined by
22 *in vitro* and *ex vivo* experiments. Although we showed that HEI3090 enhances IL-18 release
23 *in vivo* [5], it is of interest to study its impact on P2RX7 activation *in vivo*, especially since
24 HEI3090 is a promising molecule for treatment of lung cancer [5].

25 **Conclusions**

1 We described a protocol assessing P2RX7 activation *in vivo*, by taking advantage of its unique
2 property of macropore formation. Given the immunomodulatory functions of P2RX7 and the
3 increasing number of molecules aiming to modulate its activity, this protocol represents an
4 important advance in the field of purinergic signaling.

5

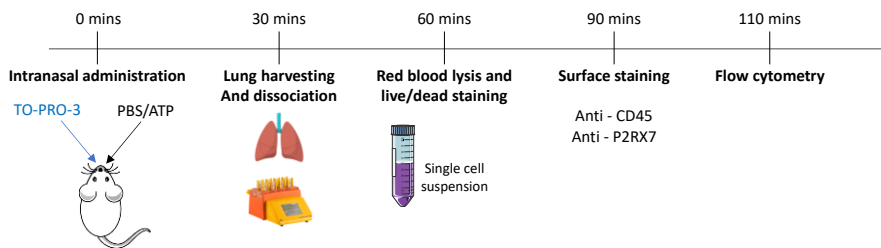
6

1 **Methods**

2 The described methods include the description of the work, along with general guidelines that
3 can be used for implementing the strategy with various compounds described to modulate
4 P2RX7 activity.

5 **Animals:** 8 weeks old WT C57BL/6J Olahsd mice are from Envigo, (Gannat, France), and 8
6 weeks old *p2rx7^{-/-}* (B6.129P2-P2rx7tm1Gab/J) backcrossed more than 10 times with WT
7 C57BL/6J Olahsd and are inbred in our animal facility. Mice were housed under
8 standardized light–dark cycles in a temperature-controlled air-conditioned environment under
9 specific pathogen-free conditions at IRCAN, Nice, France, with free access to food and water.
10 All experiments were approved by the committee for Research and Ethics of the local
11 authorities (CIEPAL #772, protocol number MESRI APAFIS #33150-2021091413316813) and
12 followed the European directive 2010/63/UE, in agreement with the ARRIVE guidelines.
13 Experiments were performed in accord with animal protection representative at IRCAN.

14 **Protocol description** is summarized in Fig. 4. Measuring P2RX7 activity *in vivo* requires 5
15 sequential and mandatory steps as illustrated below



16

17 **Fig. 4:** Schematic protocol assessing P2RX7 activity *in vivo*

18 **Time 0 - Intranasal administration**

- 19 1. Anesthetize mouse i.p. with a mixture of 25 mg/kg ketamine and 2.5 mg/kg xylazine
20 using 1 ml syringe with a 26G needle.
- 21 2. Place mouse in a box with 5% isoflurane for 1 minute.

- 1 3. When asleep, mouse is held upright and was given 25 μ l of TO-PROTM-3 (1 μ M/kg) in
2 one nostril then 25 μ l of ATP (100 mM) or 1X PBS in another using a micropipette.
3 *!\ Intranasal administration should be slow and follow the respiration rate of the mouse.*
4 *!\ Mice should be anesthetized and processed for intranasal delivery one by one.*
5 *!\ As soon as the 25 μ l+25 μ l are completely taken up by the mouse, start the 30*
6 *minutes timer.*

7 **Time 30 minutes – Mouse sacrifice and lung harvesting**

- 8 1. Sacrifice mouse by cervical elongation
9 2. Spray mouse thorax with 70% ethanol. Harvest lungs using fine and sharp scissors
10 and pliers.
11 3. Separate the lobes. Transfer the lobes into a GentleMACSTM C-tube (Miltenyi Biotech)
12 containing the enzymatic buffer for dissociation (Lung dissociation kit, Miltenyi Biotech)
13 4. Dissociate lungs using the 37_m_LDK1 program on a GentleMACSTM Octo dissociator
14 with heaters (Miltenyi Biotech)
15 5. At the end of the program, resuspend cells and pass them through a 100 μ m cell
16 strainer on top of a 50 ml tube for single cell suspensions. Wash the GentleMACSTM
17 C-tube with 1X Buffer S (Lung dissociation kit, Miltenyi Biotech) for maximum retrieval
18 of cells and pass them through the 100 μ m cell strainer.
19 6. Discard the cell strainer and centrifuge the tube at 1200 rpm 4°C for 5 minutes.
20 *!\ Keep cells in the dark at all times, and on ice except during the dissociation program.*

21 **Time 60 minutes – Red blood lysis and live/dead staining**

- 22 1. Aspirate completely the supernatant and resuspend pellet gently with 1 ml of ice-cold
23 ACK lysis buffer (Gibco) for 30 seconds to lyse red blood cells.
24 2. Add 30 ml of 1X PBS for stopping the reaction.
25 3. Centrifuge at 1200 rpm 4°C for 5 minutes
26 4. Count cells

- 1 5. Add 1 million of lung single cells in 150 µl 1X PBS in a 5 ml polypropylene tube
- 2 6. Add 150 µl of Green Live/Dead stain (2X) (Invitrogen) or 1X PBS (unstained control)
- 3 into the 5 ml polypropylene tube
- 4 *!\\ Prepare appropriate number of samples without Live/Dead staining for single-*
- 5 *stained controls*
- 6 7. Vortex and incubate in the dark at room temperature for 30 minutes
- 7 8. Add 3 ml of FACS buffer (PBS 5% FBS 0.5% EDTA) into the 5 ml polypropylene tube
- 8 9. Centrifuge at 1200 rpm 4°C for 5 minutes
- 9 10. Aspirate supernatant completely and resuspend cells in 100 µl FACS Buffer
- 10 *!\\ Keep cells in the dark at all times, and on ice unless otherwise stated.*

11 **Time 90 minutes – Surface staining**

- 12 1. Transfer cell suspension to a 96 well V plate
- 13 2. Centrifuge plate at 1300 rpm 4°C for 3 minutes
- 14 3. Flick the plate
- 15 4. Block Fc receptor using anti-CD16/32 (dil 1/100, BD Biosciences) diluted in FACS
- 16 Buffer (1X PBS, 5% FBS, 0.5% EDTA) in the dark under agitation for 10 minutes
- 17 5. Centrifuge plate at 1300 rpm 4°C for 3 minutes
- 18 6. Flick plate
- 19 7. Add antibody mix diluted in FACS buffer and homogenize immediately using a
- 20 multichannel pipette.
- 21 Antibodies: CD45 BUV395 (dil 1/100, BD Biosciences), P2RX7 PE (dil 1/8, Biolegend)
- 22 or isotype control rat IgG2b κ PE (dil 1/8, Biolegend)
- 23 *!\\ Prepare appropriate single-stained controls*
- 24 8. Incubate at 4°C in the dark under agitation for 20 minutes
- 25 9. Add 100 µl of FACS buffer per well using a multichannel pipette
- 26 10. Centrifuge plate at 1300 rpm 4°C for 3 minutes
- 27 11. Flick the plate

1 12. Resuspend cell in 100 µl of FACS buffer

2 *!!\ Keep cells in the dark at all times, and on ice.*

3 **Time 110 minutes – Flow cytometry analysis**

4 1. Cells were acquired using the CytoFLEX LX (Beckman Coulter)

5 2. Samples were analyzed using FlowJo (LLC)

6

7 **Materials**

8 1. 1 ml syringe omnifix-F (Braun, catalog number 9161406V)

9 2. 26G needle (BD Microlance 3, catalog number 304300)

10 3. Pipette

11 4. Pipette tips

12 5. Fine scissors

13 6. Sharp scissors

14 7. Pliers

15 8. GentleMACS™ C-tube (Miltenyi Biotech, catalog number 130-093-237)

16 9. 100 µm cell strainer (Falcon, catalog number 352360)

17 10. Polypropylene 50 ml tube (Falcon, catalog number 352070)

18 11. Polypropylene 5 ml tube (Falcon, catalog number 352096)

19 12. 96-well clear V bottom plates (Greiner, catalog number 651101)

20 13. Serological pipette (Falcon, catalog number 357543)

21 14. Serological pipette gun

22 15. Multi-channel pipette (Starlab, catalog number 57112-330)

23 **Reagents**

24 1. Ketamine (Virbac, catalog number 03597132111010)

- 1 2. Xylazine (Sedaxylan, Dechra, catalog number 08714225151523)
- 2 1. isoflurane / Aerrane (Baxter, catalog number DAGG9223)
- 3 2. TO-PRO™-3 (Life Technologies, catalog number T3605)
- 4 3. ATP (Sigma-Aldrich, catalog number A6419)
- 5 4. 1X Dulbecco's PBS (Gibco, catalog number 14190144)
- 6 5. 70% ethanol
- 7 6. Double distilled water
- 8 7. 20X Buffer S, enzyme D and enzyme A from the mouse lung dissociation kit (Miltenyi
- 9 Biotech, catalog number 130-095-927)
- 10 8. ACK lysis buffer (Gibco, catalog number A1049201)
- 11 9. LIVE/DEAD™ fixable green dead cell staining kit (Invitrogen, catalog number L23101)
- 12 10. Fetal bovine serum (FBS)
- 13 11. Ethylenediaminetetraacetic acid (EDTA) (Invitrogen, catalog number 15575020)
- 14 12. CD16/32 (BD Biosciences, catalog number 553141)
- 15 13. CD45 BUV395 (BD Biosciences, catalog number 564279)
- 16 14. P2RX7 PE (Biolegend, catalog number 148703)
- 17 15. Rat IgG2b κ PE (Biolegend, catalog number 400607)

18 **Equipment**

- 19 1. Anesthesia machine and box (Anesteo)
- 20 2. GentleMACS™ Octo dissociator with heaters (Miltenyi Biotech, catalog number 130-
- 21 096-427)
- 22 3. Tube and plate centrifuge (Thermofischer scientific, catalog number 75009527)
- 23 4. Plate agitator
- 24 5. CytoFLEX LX (Beckman Coulter)

25 **Reagent preparation**

26 *!\\ Prepare all reagents in sterile conditions using a PSM II tissue culture hood*

- 1 1. Anesthetics
- 2 Prepare 25 mg/kg of ketamine and 2.5 mg/kg of xylazine in 1X Dulbecco's PBS as per
- 3 250 µl of mix per 25 g of mouse.
- 4 2. Lung dissociation buffer
- 5 Dilute 20X Buffer S in double distilled water and store at 4°C. Resuspend enzyme A
- 6 and enzyme D with 1X Buffer S according to manufacturer's instructions. Add 2.4 ml
- 7 of 1X Buffer S, 15 µl of enzyme A and 100 µl of enzyme D per GentleMACS™ C-tube
- 8 (Miltenyi Biotech)
- 9 3. ATP
- 10 Prepare 100 mM stock of ATP in sterile 1X PBS, pH 6.8, aliquot and store at -80°C
- 11 *!!\ Avoid freeze/thaw cycles*
- 12 4. TO-PRO™-3
- 13 Dilute TO-PRO™-3 in 1X PBS to 1 µM/kg
- 14 *!!\ Manipulate TO-PRO™-3 in the dark*
- 15 *!!\ Aliquot TO-PRO™-3 stock and avoid freeze/thaw cycles*
- 16 5. LIVE/DEAD™ fixable green dead cell staining kit
- 17 Dilute LIVE/DEAD™ in 1X PBS to 2X working concentration per tube. Add 0.4 µL
- 18 LIVE/DEAD™ in 150µL per tube.
- 19 *!!\ Manipulate LIVE/DEAD™ green in the dark*
- 20 6. *!!\ Prepare mix of appropriate volume*
- 21 7. FACS Buffer
- 22 Prepare 500 ml of FACS Buffer containing 1X Dulbecco's PBS, 5% FBS, 0.5% EDTA
- 23 and store at 4°C
- 24 *!!\ Keep on ice at all times*
- 25 8. Antibody mix cocktail
- 26 Dilute CD45 BUV395 (dil 1/100) and P2RX7 PE (dil 1/8) or isotype control rat IgG2b κ
- 27 PE (dil 1/8) in FACS Buffer
- 28 *!!\ Keep on ice at all times and manipulate in the dark*

1 **Software**

- 2 1. CytExpert (Beckman Coulter)
- 3 2. FlowJo (LLC) or any other flow cytometry software
- 4 3. Graphpad prism

5 **Statistical analyses:**

6 All analyses were carried out using Prism software (GraphPad). Mouse experiments were
7 performed on at least $n = 5$ individuals, as indicated. Mice were equally divided for treatments
8 and controls. Data is represented as mean values and error bars represent SEM. Two-tailed
9 Mann–Whitney and unpaired t -test were used to evaluate the statistical significance between
10 groups.

11

1 **Declarations**

2 **Author's contribution:**

3 S.J.H. and V.V.-C. conceived and designed the study. S.J.H. developed the methodology.
4 S.J.H, T.J. and V.V.-C. acquired the data (provided animals, provided facilities, and so on).
5 S.J.H, P.H. and V.V.-C. analyzed and interpreted the data. S.J.H. and V.V.-C. wrote the
6 manuscript. All authors reviewed the manuscript.

7 **Funding:** This research was funded by the association for the research on cancer,
8 France (ARC), the French Government (National Research Agency, ANR through the
9 "Investments for the Future": program reference #ANR-11-LABX-0028-01), SJH is
10 funded by the "Ligue Nationale Contre le Cancer" and the "Fondation pour la
11 Recherche Médicale" grant number #FDT202106013099 and ARC (grant number
12 ARCTHEM2021020003478).

13 **Acknowledgements:** The authors thanks members of the COST PRESTO (CA21130) for
14 valuable discussion.

15 **Availability of data and materials:** All data generated and analyzed during this study are
16 included in this article and its supplementary files

17 **Ethics Approval:** All experiments were approved by the committee for Research and Ethics
18 of the local authorities (CIEPAL #772, protocol number MESRI APAFIS #33150-
19 2021091413316813) and followed the European directive 2010/63/UE, in agreement with
20 the ARRIVE guidelines.

21 **Consent to participate:** not applicable

22 **Consent for publication:** not applicable

23 **Competing interests:** the authors declare that they have no competing interests

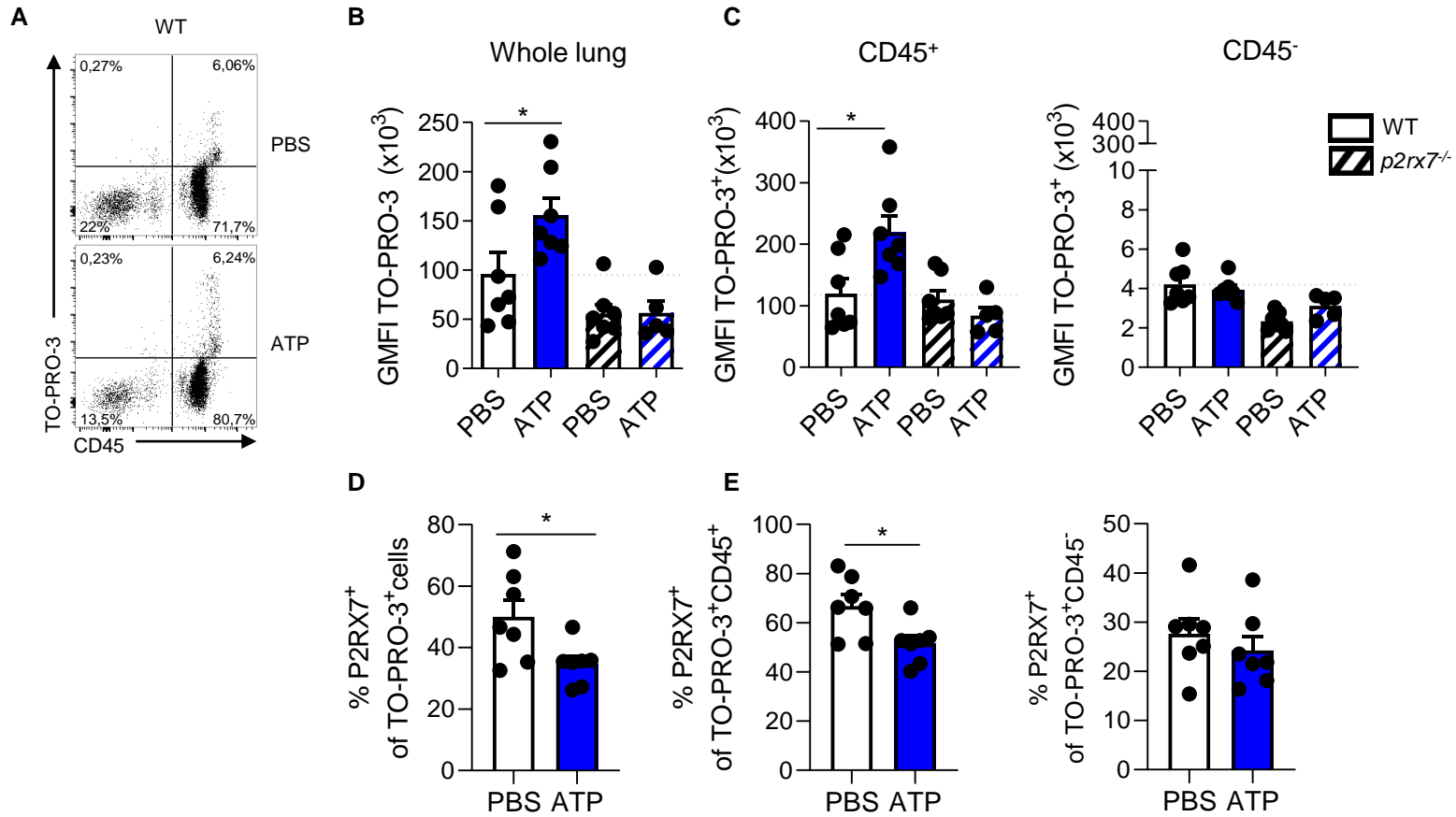
24

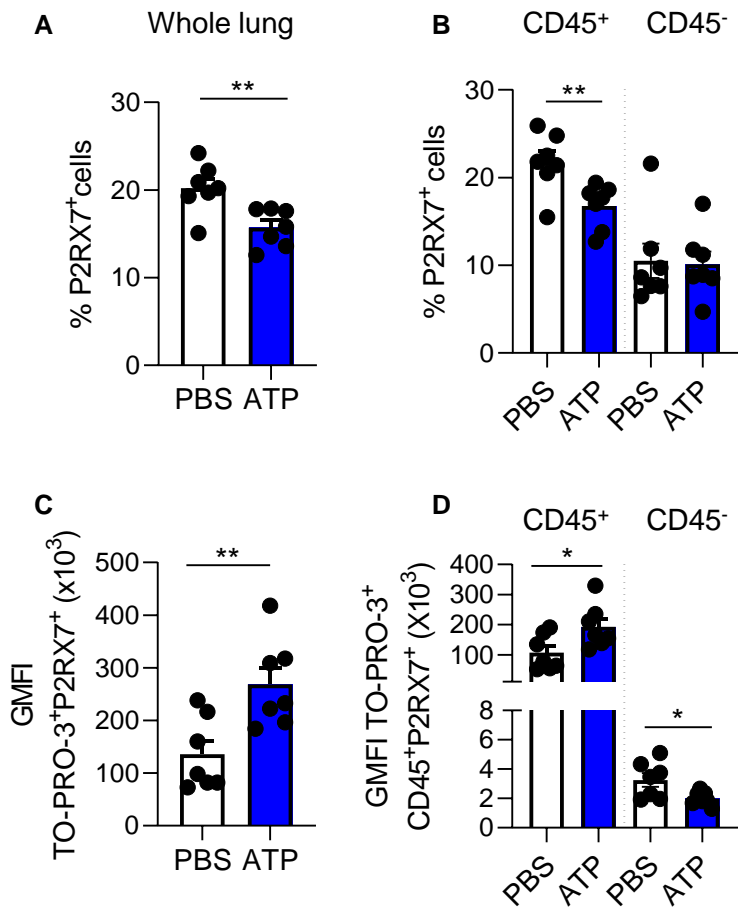
1 References

- 2 1. Pellegatti P, Raffaghello L, Bianchi G, Piccardi F, Pistoia V, di Virgilio F. Increased level of
3 extracellular ATP at tumor sites: in vivo imaging with plasma membrane luciferase. *PLoS*
4 *One*. 2008;3:e2599.
- 5 2. Kopp R, Krautloher A, Ramírez-Fernández A, Nicke A. P2X7 Interactions and Signaling –
6 Making Head or Tail of It. *Front Mol Neurosci*. 2019;12.
- 7 3. Surprenant A, Rassendren F, Kawashima E, North RA, Buell G. The cytolytic P2Z receptor
8 for extracellular ATP identified as a P2X receptor (P2X7). *Science*. 1996;272:735–8.
- 9 4. Perregaux DG, McNiff P, Laliberte R, Conklyn M, Gabel CA. ATP acts as an agonist to
10 promote stimulus-induced secretion of IL-1 beta and IL-18 in human blood. *J Immunol*.
11 2000;165:4615–23.
- 12 5. Douguet L, Janho D, Hreich S, Benzaquen J, Seguin L, Juhel T, Dezitter X, et al. A small-
13 molecule P2RX7 activator promotes anti-tumor immune responses and sensitizes lung
14 tumor to immunotherapy. *Nat Commun*. 2021;12:653.
- 15 6. Homerin G, Jawhara S, Dezitter X, Baudelet D, Dufrénoy P, Rigo B, et al. Pyroglutamide-
16 Based P2X7 Receptor Antagonists Targeting Inflammatory Bowel Disease. *J Med Chem*.
17 2020;63:2074–94.
- 18 7. Gondé H, Demeules M, Hardet R, Scarpitta A, Junge M, Pinto-Espinoza C, et al. A
19 Methodological Approach Using rAAV Vectors Encoding Nanobody-Based Biologics to
20 Evaluate ARTC2.2 and P2X7 In Vivo. *Front Immunol*. 2021;12:704408.
- 21 8. di Virgilio F, Schmalzing G, Markwardt F. The Elusive P2X7 Macropore. *Trends Cell Biol*.
22 2018;28:392–404.
- 23 9. Ou A, Gu BJ, Wiley JS. The scavenger activity of the human P2X7 receptor differs from
24 P2X7 pore function by insensitivity to antagonists, genetic variation and sodium
25 concentration: Relevance to inflammatory brain diseases. *Biochim Biophys Acta Mol Basis*
26 *Dis*. 2018;1864:1051–9.
- 27 10. Kubick C, Schmalzing G, Markwardt F. The effect of anions on the human P2X7 receptor.
28 *Biochim Biophys Acta*. 2011;1808:2913–22.
- 29 11. Inquimbert P, Bartels K, Babaniyi OB, Barrett LB, Tegeder I, Scholz J. Peripheral nerve
30 injury produces a sustained shift in the balance between glutamate release and uptake in
31 the dorsal horn of the spinal cord. *Pain*. 2012;153:2422–31.
- 32 12. Barczyk A, Bauderlique-Le Roy H, Jouy N, Renault N, Hottin A, Millet R, et al. Flow
33 cytometry: An accurate tool for screening <sc>P2RX7</sc> modulators. *Cytometry Part A*.
34 2021;99:793–806.
- 35 13. Feng Y-H, Wang L, Wang Q, Li X, Zeng R, Gorodeski GI. ATP stimulates GRK-3
36 phosphorylation and beta-arrestin-2-dependent internalization of P2X7 receptor. *Am J*
37 *Physiol Cell Physiol*. 2005;288:C1342-56.
- 38 14. Hiken JF, Steinberg TH. ATP downregulates P2X7 and inhibits osteoclast formation in
39 RAW cells. *Am J Physiol Cell Physiol*. 2004;287:C403-12.
- 40 15. Young CNJ, Chira N, Róg J, Al-Khalidi R, Benard M, Galas L, et al. Sustained activation of
41 P2X7 induces MMP-2-evoked cleavage and functional purinoceptor inhibition. *J Mol Cell*
42 *Biol*. 2018;10:229–42.
- 43 16. Kanellopoulos JM, Almeida-da-Silva CLC, Rüütel Boudinot S, Ojcius DM. Structural and
44 Functional Features of the P2X4 Receptor: An Immunological Perspective. *Front Immunol*.
45 2021;12:645834.

- 1 17. Müller T, Vieira RP, Grimm M, Dürk T, Cicko S, Zeiser R, et al. A potential role for P2X7R
2 in allergic airway inflammation in mice and humans. *Am J Respir Cell Mol Biol.* 2011;44:456–
3 64.
- 4 18. Lucattelli M, Cicko S, Müller T, Lommatzsch M, de Cunto G, Cardini S, et al. P2X7
5 receptor signaling in the pathogenesis of smoke-induced lung inflammation and
6 emphysema. *Am J Respir Cell Mol Biol.* 2011;44:423–9.
- 7 19. Riteau N, Gasse P, Fauconnier L, Gombault A, Couegnat M, Fick L, et al. Extracellular ATP
8 is a danger signal activating P2X7 receptor in lung inflammation and fibrosis. *Am J Respir Crit*
9 *Care Med.* 2010;182:774–83.
- 10 20. Baxter M, Eltom S, Dekkak B, Yew-Booth L, Dubuis ED, Maher SA, et al. Role of transient
11 receptor potential and pannexin channels in cigarette smoke-triggered ATP release in the
12 lung. *Thorax.* 2014;69:1080–9.
- 13 21. Monção-Ribeiro LC, Faffe DS, Santana PT, Vieira FS, da Graça CLAL, Marques-da-Silva C,
14 et al. P2X7 receptor modulates inflammatory and functional pulmonary changes induced by
15 silica. *PLoS One.* 2014;9:e110185.
- 16 22. Eltom S, Stevenson CS, Rastrick J, Dale N, Raemdonck K, Wong S, et al. P2X7 receptor
17 and caspase 1 activation are central to airway inflammation observed after exposure to
18 tobacco smoke. *PLoS One.* 2011;6:e24097.
- 19 23. Benzaquen J, Dit Hreich SJ, Heeke S, Juhel T, Lalvee S, Bauwens S, et al. P2RX7B is a new
20 theranostic marker for lung adenocarcinoma patients. *Theranostics.* 2020;10:10849–60.
- 21 24. Mishra A, Chintagari NR, Guo Y, Weng T, Su L, Liu L. Purinergic P2X7 receptor regulates
22 lung surfactant secretion in a paracrine manner. *J Cell Sci.* 2011;124:657–68.
- 23 25. Benzaquen J, Heeke S, Janho Dit Hreich S, Douguet L, Marquette CH, Hofman P, et al.
24 Alternative splicing of P2RX7 pre-messenger RNA in health and diseases: Myth or reality?
25 *Biomed J.* 2019;42:141–54.
- 26 26. Kido Y, Kawahara C, Terai Y, Ohishi A, Kobayashi S, Hayakawa M, et al. Regulation of
27 activity of P2X7 receptor by its splice variants in cultured mouse astrocytes. *Glia.*
28 2014;62:440–51.
- 29 27. Kochukov MY, Ritchie AK. P2X7 receptor stimulation of membrane internalization in a
30 thycocyte cell line. *J Membr Biol.* 2005;204:11–21.
- 31 28. Qu Y, Dubyak GR. P2X7 receptors regulate multiple types of membrane trafficking
32 responses and non-classical secretion pathways. *Purinergic Signal.* 2009;5:163–73.
- 33 29. Arguin G, Bourzac J-F, Placet M, Molle CM, Paquette M, Beaudoin J-F, et al. The loss of
34 P2X7 receptor expression leads to increase intestinal glucose transit and hepatic steatosis.
35 *Sci Rep.* 2017;7:12917.
- 36 30. Amadio S, Parisi C, Piras E, Fabbriozio P, Apolloni S, Montilli C, et al. Modulation of P2X7
37 Receptor during Inflammation in Multiple Sclerosis. *Front Immunol.* 2017;8:1529.
- 38 31. Chagnon F, Fournier C, Charette PG, Moleski L, Payet MD, Dobbs LG, et al. In vivo
39 intravital endoscopic confocal fluorescence microscopy of normal and acutely injured rat
40 lungs. *Lab Invest.* 2010;90:824–34.
- 41 32. Kanou T, Ohsumi A, Kim H, Chen M, Bai X, Guan Z, et al. Inhibition of regulated necrosis
42 attenuates receptor-interacting protein kinase 1-mediated ischemia-reperfusion injury after
43 lung transplantation. *J Heart Lung Transplant.* 2018;37:1261–70.
- 44 33. Unal Cevik I, Dalkara T. Intravenously administered propidium iodide labels necrotic cells
45 in the intact mouse brain after injury. *Cell Death Differ.* 2003;10:928–9.

- 1 34. Whalen MJ, Dalkara T, You Z, Qiu J, Bempohl D, Mehta N, et al. Acute plasmalemma
2 permeability and protracted clearance of injured cells after controlled cortical impact in
3 mice. *J Cereb Blood Flow Metab.* 2008;28:490–505.
- 4 35. Tsurusaki S, Kanegae K, Tanaka M. In Vivo Analysis of Necrosis and Ferroptosis in
5 Nonalcoholic Steatohepatitis (NASH). *Methods Mol Biol.* 2022;2455:267–78.
- 6
- 7





SUPP

